

Alma Mater Studiorum Università di Bologna  
Archivio istituzionale della ricerca

Combined effect of atmospheric gas plasma and UVA light: A sustainable and green alternative for chemical decontamination and microbial inactivation of fish processing water

This is the final peer-reviewed author's accepted manuscript (postprint) of the following publication:

*Published Version:*

Zorzi V., Berardinelli A., Gozzi G., Ragni L., Vannini L., Ceccato R., et al. (2023). Combined effect of atmospheric gas plasma and UVA light: A sustainable and green alternative for chemical decontamination and microbial inactivation of fish processing water. CHEMOSPHERE, 317(March 2023), 1-8 [10.1016/j.chemosphere.2023.137792].

*Availability:*

This version is available at: <https://hdl.handle.net/11585/940814> since: 2023-09-07

*Published:*

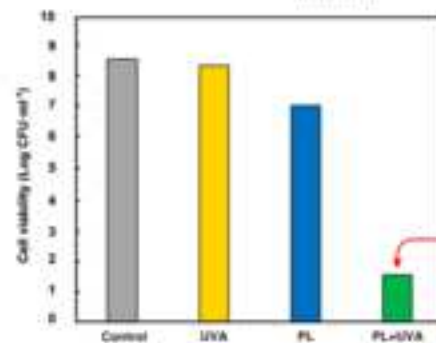
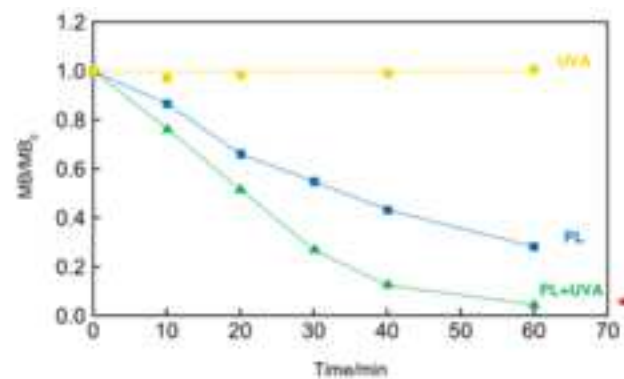
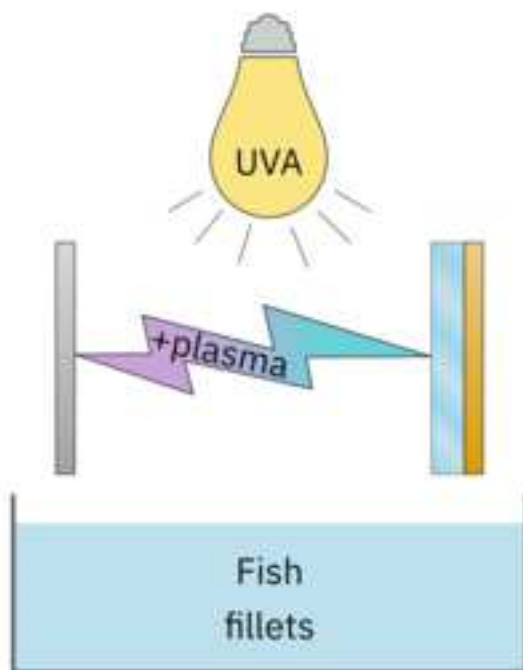
DOI: <http://doi.org/10.1016/j.chemosphere.2023.137792>

*Terms of use:*

Some rights reserved. The terms and conditions for the reuse of this version of the manuscript are specified in the publishing policy. For all terms of use and more information see the publisher's website.

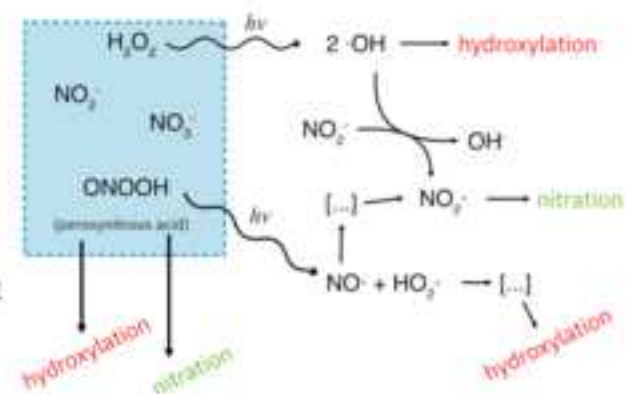
This item was downloaded from IRIS Università di Bologna (<https://cris.unibo.it/>).  
When citing, please refer to the published version.

(Article begins on next page)



Combined process:  
enhanced  
decontamination  
& microbial  
inactivation

**Mechanism:** photoactive species  
in plasma-activated water



## **Highlights**

- Cold plasma is a chlorine-free technique for water decontamination and disinfection.
- Coupling cold plasma with UVA irradiation leads to process intensification.
- Synergy explained by the presence of photoactive species in plasma-activated water.
- The treatment does not affect the quality of the food.

# Combined effect of atmospheric gas plasma and UVA light: a sustainable and green alternative for chemical decontamination and microbial inactivation of fish processing water

Vittorio Zorzi<sup>a</sup>, Annachiara Berardinelli<sup>a,b</sup>, Giorgia Gozzi<sup>c</sup>, Luigi Ragni<sup>c,d</sup>, Lucia Vannini<sup>c,d</sup>,  
Riccardo Ceccato<sup>a</sup>, Francesco Parrino<sup>a\*</sup>

<sup>a</sup> Department of Industrial Engineering, University of Trento, Via Sommarive 9, 38123 Trento, Italy

<sup>b</sup> Center Agriculture Food Environment – C3A, University of Trento, Via E. Mach 1, 38010 S. Michele all’Adige (TN), Italy

<sup>c</sup> Department of Agricultural and Food Sciences, Alma Mater Studiorum, University of Bologna, P.zza Goidanich 60, Cesena (FC), Italy

<sup>d</sup> Inter-Departmental Centre for Agri-Food Industrial Research, Alma Mater Studiorum, University of Bologna, Via Q. Bucci 336, Cesena (FC), Italy

\* Corresponding author

## Abstract

The simultaneous use of UVA light irradiation coupled with low energy cold plasma generated by a dielectric barrier discharge prototype, results in significant enhancement of efficiency of the integrated process with respect to the sole plasma treatment. This effect has been demonstrated both on microbial inactivation of a food-borne pathogen, i.e. *Listeria monocytogenes*, and on the degradation of a compound of biological origin such as phenylalanine. In the latter case, the analysis of its reaction intermediates and the spectroscopic identification and quantification of peroxynitrites, allowed to propose mechanistic hypotheses on the nature of the observed synergistic effects.

Moreover, it has been demonstrated that the process does not affect the quality of trout fillets, indicating its suitability as a chlorine-free, green, and sustainable tool for the decontamination of fish processing water.

**Keywords:** Food processing water, UVA light; dielectric barrier discharge; process intensification; microbial inactivation; peroxynitrite.

## 1. Introduction

Fish products represents an important source of both macro and micro nutrients for human consumption, and are considered essential to meet the increasing demand of high valuable protein and long chain omega 3 (n-3) polyunsaturated fatty acids (PUFA) (Sampels, 2014).

Due to its structure and composition, fish is a highly perishable product, which requires careful processing in order to prolong the shelf life and to limit losses. Therefore, fish handling has a big role, from catching and along the supply chain until packaging and eventually human consumption, in the preservation of nutritional properties and hygienic conditions, and in the reduction of postharvest losses (Sefa-Dedeh, 2003).

To this aim, during various stages of processing a high amount of water is required (Murali et al., 2021). Generally, from 5 to 11 m<sup>3</sup> water per ton of fish intake are required for fish filleting and 15 m<sup>3</sup> for canning (Unep, 1999). These operations, in addition to plant cleaning procedures, also generate significant wastewater, which must be, in turn, subjected to treatment processes ruled by stringent liquid effluent regulations (Chowdhury et al., 2010).

Several green technologies such as photocatalysis and ozonation have been proposed for water treatment purposes (Miklos et al., 2018) but their large-scale application is still limited (Wang et al., 2021; Wang et al., 2022). On the other hand, sanitizers are used in industry to assure the microbial quality of the washing water, and to avoid cross contamination. For instance, based on its efficacy towards bacteria, chlorine was extensively employed in different food processing units, from fruits

51 and vegetables to meat. However, the chemical risk associated with the formation and accumulation,  
52 both in process water and products, of chlorine disinfection intermediates such as trichloromethane  
53 and other carcinogenic and mutagenic chlorinated compounds, (EFSA Journal, 2019) is of great  
54 concern. For this reason, the use of chlorine is now prohibited in several European countries (Gil et  
55 al., 2009).

56 Among the novel techniques proposed to tackle this issue, “cold plasma” produced under atmospheric  
57 conditions allows to inactivate pathogenic agents and to decontaminate water, due to formation of  
58 strong oxidants such as ozone (O<sub>3</sub>) and reactive oxygen (ROS) and nitrogen (RNS) species produced  
59 when air acts as the working gas (Oehmigen et al., 2010; Berardinelli et al., 2016). These reactive  
60 species are responsible of cell membrane damages, which further enable cell penetration, consequent  
61 DNA damages, and eventually death of the pathogen microorganism (Bourke et al., 2017). It is known  
62 that reactive molecules production is affected by the applied energy level, the nature of the gas  
63 mixture used to generate the discharge, (Moreau et al., 2008) while the characteristics of the substrate  
64 and the microorganism type, load, and physiological state highly affect the efficacy of the treatment  
65 (Berardinelli et al., 2012; Guo et al., 2015). In particular, the decontamination efficacy of the  
66 atmospheric gas plasma technique was evidenced towards Gram-negative and Gram-positive  
67 bacteria, spores, yeasts, molds, and viruses (Montie et al., 2000).

68 Differently from other food sectors, few studies have been dedicated to the application of this non-  
69 thermal treatment for the processed fish. The bactericidal effect of a dielectric barrier discharge  
70 (DBD) prototype was evidenced in mackerel fillets by Trevisani et al. (2021) in terms of viability and  
71 histamine-producing activity of psychrotrophic bacteria, also in combination with sodium dodecyl  
72 sulphate and lactic acid. The potentiality of the technique for ensuring the microbiological quality  
73 and safety of seafood have been recently evidenced in the reviews proposed by Kulawik and Kumar  
74 Tiwari (2018), Ekonomou and Boziaris (2021), and Andoni et al. (2021).

75 If cold plasma reactive species generated in gas phase can diffuse into a water-based environment or  
76 can be generated underwater, a series of complex reactions involving the formation of biologically  
77 active species such as nitric/nitrous acid, hydrogen peroxide ( $\text{H}_2\text{O}_2$ ), superoxide radical anion ( $\text{O}_2^{\cdot-}$ ),  
78 and peroxyxynitrite ion ( $\text{ONOO}^-$ ) or peroxyxynitrous acid ( $\text{ONOOH}$ ) can occur (Oehmigen et al., 2010).  
79 However, the interaction between gas and liquid phases or the underwater generation of these species  
80 is not well understood (Jiang et al., 2016) and require further fundamental investigation.

81 The use of UVC light (wavelength,  $\lambda$ , ranging between 100 and 280 nm), also known as “cold  
82 pasteurization” is another well-established method to reduce or eliminate pathogens and to extend the  
83 shelf life of fresh-cut fruits and vegetables. However, UVC light is highly energetic and represents  
84 an expensive investment in terms of both initial set-up and operating costs. Irradiation at lower energy  
85 (such as UVA, with  $\lambda$  between 320 and 400 nm) would be desirable, but generally ineffective for the  
86 required tasks (EPA Research, 2016). In a previous paper (Berardinelli et al. 2021), we investigated  
87 the features of a treatment combining cold plasma discharge and photocatalysis for water  
88 decontamination in order to assess the existence of process intensification between the two  
89 technologies, similarly to other cases in the relevant literature. Preliminary results suggested that  
90 afterglow species, e.g. hydrogen peroxide and/or peroxyxynitrous acid could be activated by UVA light  
91 irradiation, producing hydroxyl radicals in the liquid phase and that  $\text{TiO}_2$  limited this effect by acting  
92 as UVA screen barrier material. Even if the decontamination efficiency of photocatalysis under  
93 certain conditions could be higher than that obtained with plasma systems, no synergistic effects  
94 between plasma and photocatalysis could be proved in this case.

95 In the present paper, we focus at providing novel insights on the synergistic effect between plasma  
96 and UVA irradiation, reported in our previous study for methylene blue as a model pollutant, and to  
97 extend it for a compound of biological origin such as phenylalanine, and for bacterial inactivation.  
98 The identification and quantification of active species such as peroxyxynitrous acid and the detection  
99 of particular reaction intermediates in plasma activated water, allowed us to propose some

100 mechanistic hypotheses on the nature of the observed synergistic effects, which is still under debate  
101 in literature. Finally, tests on microbial inactivation of a food-borne pathogen and on the quality of  
102 fish fillets subjected to the integrated process have been carried out, in order to highlight possible  
103 changes in colors and sensorial attributes of the fish flesh. The information hereby presented, deriving  
104 from interdisciplinary but complementary research efforts, indicates that the combination of cold  
105 plasma and UVA irradiation could be suggested as a sustainable and chlorine-free tool for the  
106 decontamination of fish processing water.

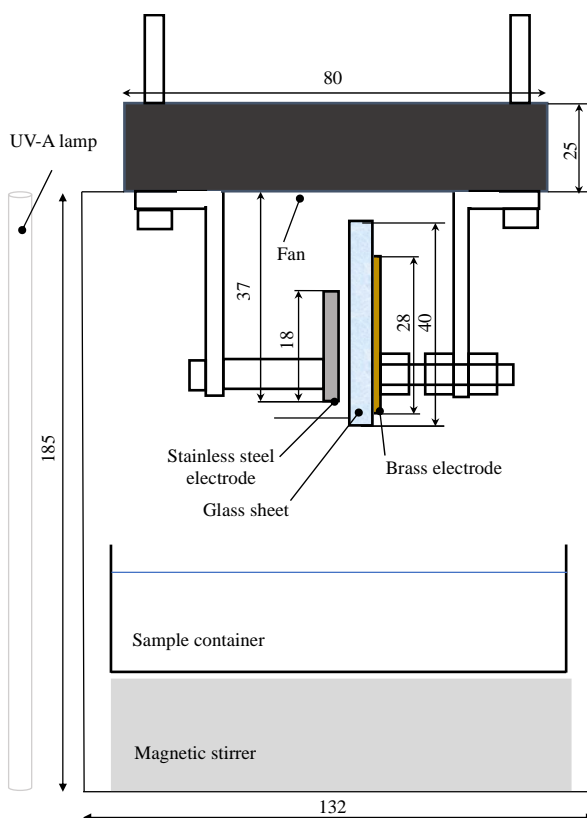
107



## 108 2. Materials and methods

### 109 2.1 Experimental set-up

110 The dielectric barrier discharge (DBD) gas plasma device consisted of two parallel plate electrodes  
 111 made of brass ( $28\text{ mm} \times 15\text{ mm} \times 2\text{ mm}$ ) and stainless steel ( $10\text{ mm} \times 18\text{ mm} \times 1.5\text{ mm}$ ), respectively.  
 112 The brass electrode was covered by a thin sheet of glass ( $30\text{ mm} \times 40\text{ mm} \times 5\text{ mm}$ ) working as  
 113 dielectric barrier. A fan was mounted at about 40 mm over the electrodes in order to facilitate the  
 114 transport of the plasma induced species to the reacting solution. The solution (200 mL) was contained  
 115 in a cylindrical reactor (inner diameter 120 mm; height 60 mm) made of Pyrex, placed within the  
 116 chamber, and the free surface was at about 20 mm below the discharge (filling height of the reactor  
 117 about 3 cm) (Fig. 1).



118 **Fig. 1.** Scheme of the experimental set up consisting of the dielectric barrier discharge (DBD) device  
 119 in a Pyrex chamber surrounded by UVA lamps.  
 120

121

122 The electrodes, the fan, the reacting medium and the stirrer were confined in a Pyrex chamber (132  
123 mm × 185 mm) externally irradiated by means of six actinic Mercury UVA lamps (Philips, nominal  
124 power 14 W each, emission peak centered at 365 nm as shown in Fig. S1, radiation power absorbed  
125 per unit volume of the solution about 0.7 mW mL<sup>-1</sup>) surrounding the chamber in hexagonal geometry.  
126 High voltage transformers and power switching transistors supplied by a stabilized DC power supply  
127 (Elektro-Automatik GmbH & Co.KG, EA-PS 2042-06B) were used to drive the discharge operating  
128 at 19.15 V (3.15 ± 0.5 A) and by using air as working gas. The voltage output was characterized by  
129 a like-shaped sinusoidal waveform with a peak to peak value of 13.8 kV (fundamental frequency of  
130 oscillation around 12.7 kHz). The gas plasma device absorbed around 60 W (the active power at the  
131 electrode is around 17 W).

132 After 10 minutes of plasma treatment the temperature inside the glass chamber reached 33 ± 1°C  
133 (starting from ca. 26 °C) and was constant during the treatment (by coupling plasma with UVA, a  
134 small temperature increases of about 3°C was measured at the end of treatment). Ozone production  
135 within the chamber in the presence of the discharge has been elsewhere reported (about 0.017 mg L<sup>-1</sup>  
136 <sup>1</sup> in the gas phase after 2.5 min of discharge duration in a 0.19 m<sup>3</sup> volume chamber) as well as the  
137 nitrites (95 mg L<sup>-1</sup>) and nitrates (7.5 mg L<sup>-1</sup>) levels after 60 minutes in a 150 mL of 0.9% NaCl  
138 deionized water (Ragni et al., 2016).

139

## 140 2.2 Microbiological tests

141 Microbiological tests were performed in Petri dishes (90 mm of diameter) containing 26 milliliters of  
142 a cell suspension (filling height: 0.6 cm) of a 20-hours old culture of *Listeria monocytogenes* 56Ly,  
143 previously centrifuged and resuspended in saline solution (0.9% w/v) (final cell load of 8.66 ± 0.33  
144 Log CFU mL<sup>-1</sup>).

145 Cell viability and the pH of the cell suspensions were evaluated immediately after 60 minutes of each  
146 treatment (performed without stirring the samples) by plate counting onto agarized Brain Heart  
147 Infusion media (Oxoid) and by a pH-meter Meter Basic 20 (Crison), respectively. Each treatment was

performed in triplicate and samples analyzed in duplicate. Data are expressed as means and standard deviations. Microbiological inactivation and chemical degradation tests were carried out for (i) gas plasma treatment, (ii) UVA light irradiation, and (iii) integrated gas plasma and UVA light process.

### 2.3 Phenylalanine and methylene blue degradation

The degradation tests of phenylalanine (Sigma-Aldrich, p.a.) and methylene blue (Sigma-Aldrich, p.a.) were carried out at an initial concentration of 1 mM and 0.025 mM, respectively. The solution was stirred inside the reactor for 10 minutes and then the plasma discharge and/or UVA light were turned on. Three test sets were carried out, in the presence of plasma only, only under UVA irradiation, and under simultaneous plasma and UVA irradiation. Each test was carried out three times and the deviation of each experimental point was within  $\pm 5\%$ . Samples were taken at regular intervals of time by using a syringe, and analyzed by means of a HPLC Shimadzu Prominence equipped with a Shimpack GWS C18, 5  $\mu\text{m}$ ,  $150 \times 4.6$  mm column and a diode array UV-vis detector. The eluent was a mixture of 95% aqueous buffer solution (monosodium phosphate/ disodium phosphate) and 5% acetonitrile by volume, circulating at a flow rate of  $1 \text{ mL min}^{-1}$ . The quantification of the reaction intermediates was performed through calibration, by using standards (pro analysis grade) purchased from Sigma-Aldrich.

### 2.4 Quantification of peroxyxynitrous acid

The amount of peroxyxynitrous acid generated in bidistilled water has been measured under sole UVA irradiation, sole plasma discharge, and integrated plasma and UVA irradiation. By taking into account that the pH of the plasma activated water solution decreases to ca. 3 after ca. 10 minutes from switching on the discharge, and that the pKa of peroxyxynitrous acid is reported to be 6.8 (Pryor and Squadrito, 1995), peroxyxynitrous acid is present in the plasma activated water in its protonated form. However, the latter is highly reactive and needs to be stabilized before spectroscopic quantification. To this aim, and to avoid the uncertainties associated with a manual operation, the apparatus hereby

described and schematized in the Supporting Information (Fig. S2) has been devised. The reacting solution was transferred through a tube (inner diameter 0.5 mm) by means of a vacuum pump to a two neck round flask sealed with a rubber cap, containing 1 mL of NaOH solution (pH = 12.5). In this way a controlled amount of reacting solution could be sampled and immediately mixed with a NaOH solution in a reproducible way. The sample was then collected and analysed by means of an UV-9000 Shimadzu UV-vis spectrophotometer. The same procedure was then repeated at fixed intervals of time during the run. UV-vis spectra were deconvoluted by means of Origin software (2022) to correctly evaluate the concentration of peroxynitrite through Lambert Beer law, by considering a molar extinction coefficient at 302 nm of  $1670 \text{ L mol}^{-1} \text{ cm}^{-1}$  (Hughes and Nicklin, 1968). The fitting of the spectra was satisfactory, as shown in Fig. S3 in the Supporting Information.

## 2.5 Fish fillet quality assessment

In order to assess possible negative effects of the proposed treatments on fish quality properties, fresh rainbow trout fillets (*Oncorhynchus mykiss*) were purchased from a local producer in the Trentino province (Italy).

Fish fillet samples (about 40 mm × 30 mm) were obtained from a total of 10 fillets. 12 samples were treated with gas plasma and 12 samples with integrated gas plasma and UVA light process for 60 minutes (for both treatments). The tests were performed in a cylindrical reactor (inner diameter 120 mm; height 60 mm) in Pyrex positioned within the above described chamber and containing 200 mL of distilled water. A number of 12 non-treated fillets immersed for 60 min in distilled water was also considered as control samples. For each treatment type, quality properties were assessed on 12 fillet samples before and immediately after the treatments, and at 1, 3 and 5 days of storage at 4°C. Color measurements of the pulp were conducted by means of a Minolta ChromaMeter CR-400 reflectance colorimeter (Minolta, Milan, Italy). For each acquisition, an average value of three measurements was calculated. According to the CIELab system,  $L^*$ ,  $a^*$  and  $b^*$  coordinates were analyzed (CIE, 1976) and the Chroma values were calculated as  $C^* = \sqrt{a^{*2} + b^{*2}}$ .

On the same fillet fish samples, a sensory evaluation was conducted by means of a trained sensory panel according to a method developed by Cárdenas Bonilla et al. (2007) for fresh cod *Gadus morhua* fillets and adapted for trout fillet (Table 1). Increments in the demerit score refer to increments in the fish deterioration.

**Table 1.** Demerit score scheme for sensory evaluation.

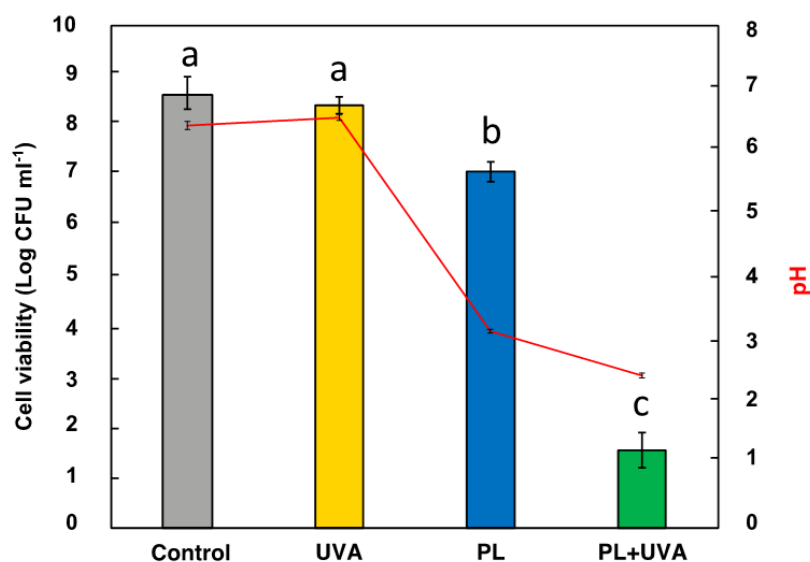
Flesh quality parameter	Description	Demerit score
<b>Texture</b>	Firm	0
	Rather soft	1
	Very soft	2
<b>Odour</b>	Fresh, neutral	0
	Seaweed, marine, grass	1
	Sour milk	2
	Acetic, ammonia	3
<b>Colour</b>	White, greyish	0
	Some yellowish, a little pinkish	1
	Yellow, over all pink	2
<b>Bright</b>	Transparent, bluish	0
	Opaque	1
	Milky	2
Range of the total demerit scores		(0-9)

Within the same treatment, possible significant differences in color attributes ( $L^*$  and  $C^*$ ) were identified before, after the treatment, and during the storage by the analysis of variance (ANOVA) and Post Hoc Tukey. For demerit scores, the same significant differences were explored by Kruskal-Wallis test followed by Dwass-Steel-Critchlow-Fligner pairwise comparisons (jamovy Desktop, ver. 2.2.5).

### 214 3. Results and discussion

215 Fig. 2 reports cell counts of *Listeria monocytogenes* 56Ly following UVA, plasma and the combined  
 216 treatment, along with the results of a control experiment.

217



218

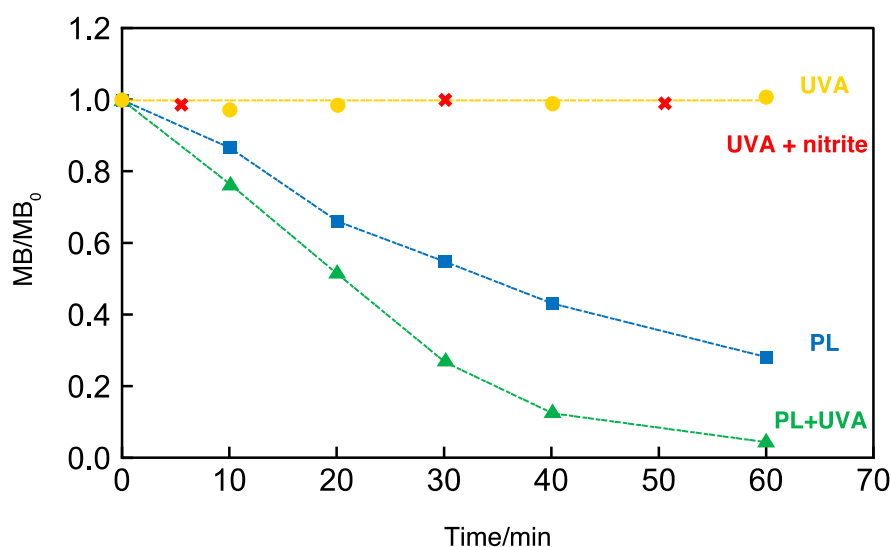
219 **Fig. 2.** Cell viability of *Listeria monocytogenes* 56Ly cells in saline solution and pH values of the  
 220 solutions after exposure for 60 min to UV light (UVA), cold plasma (PL), and integrated UV light –  
 221 cold plasma (PL + UVA) treatments. Values represent means  $\pm$  standard deviations of values from  
 222 three separate experiments. Different letters indicate significant differences among treatments ( $p <$   
 223 0.05, ANOVA, post hoc Tukey).

224

225 While UVA irradiation for 60 minutes was ineffective in decreasing cell viability, exposure to plasma  
 226 discharge had a significant ( $p < 0.05$ ) effect resulting in 1.4 Log unit inactivation. By contrast, when  
 227 the UVA light and plasma were simultaneously applied, the overall effect was remarkably enhanced,  
 228 thus showing a synergistic effect of the combined treatments. In fact, the level of surviving cells did  
 229 not exceed 1.5 Log CFU mL<sup>-1</sup> being the Log reductions increased by four times compared to the  
 230 plasma alone.

231 As reported in Fig. 2, acidification of the solution occurred during plasma treatment. However, as  
232 widely recognized in literature, the pH decrease does not influence the viability of the microbial cells  
233 (Dezest et al., 2017). Similarly, literature reports confirm that the sole UV irradiation does not play a  
234 major role in microbial inactivation process, at least when air is used as the operating gas (Guo et al.,  
235 2015; Probst-Rüd et al., 2017), as in the present case. To enhance UVA efficacy against different  
236 food-borne pathogens some authors successfully tested its use in combination with chemicals  
237 including silver ions, antimicrobials and food preservatives (curcumin, acetic or fumaric acids), thus  
238 ensuring safety of food and waters (Jeon and Ha, 2020). A synergistic interaction when treating  
239 bacterial suspensions of *Escherichia coli* with high-power plasma followed by UVA treatment was  
240 reported also by Pavlovich et al. (2013) Authors identify nitrite ions as the most important plasma-  
241 associated species responsible for the synergistic effect. In order to test this hypothesis in a more  
242 controllable way, i.e. to avoid the biological effects of the nitrite ions on the cells, we performed the  
243 degradation of methylene blue (MB) under sole UVA irradiation and UVA in the presence of nitrite  
244 ions (1 mM). It is worth to mention that MB was chosen because it is a widely used model pollutant  
245 whose photochemical behavior and photodegradation path is well known. Moreover, it presents an  
246 absorption minimum between 350 and 450 nm, i.e. at the maximum emission (365 nm) of the  
247 irradiation source hereby used. Therefore, photoinduced processes driven by its excited triplet state  
248 such as photosensitized singlet oxygen generation are minimized (Mitoraj et al., 2018). Results are  
249 reported in Fig. 3, along with the MB degradation under sole plasma and coupled plasma-UVA  
250 treatments.

251



252

253 **Fig. 3.** Normalized concentration of methylene blue (MB) during UVA light (UVA, circles), UV light  
 254 in the presence of 1 mM sodium nitrite (UVA+nitrite, X marks), cold plasma (PL, squares), and  
 255 integrated UVA light – cold plasma (PL + UVA, triangles) treatment. Each reaction was performed  
 256 three times and the standard deviation was  $\pm 5\%$ . Significant differences among treatments were  
 257 observed at each treatment time ( $p < 0.05$ , Mann-Whitney test).

258

259 UVA light does not result in degradation of MB both in the presence and in the absence of nitrite  
 260 ions. Therefore, the synergistic effect observed in UVA irradiated plasma activated water, cannot be  
 261 ascribed to the sole presence of nitrite ions. Notably, the synergistic effect observed for the biological  
 262 tests is also taking place for the MB degradation. In fact, in the presence of the plasma discharge and  
 263 in the absence of external irradiation, the concentration of MB decreases reaching 44% degradation  
 264 after 30 minutes. On the other hand, MB degradation almost doubled (ca. 73%) after the same time  
 265 when the solution was simultaneously irradiated. Also in this case, the pH of the solution decreased  
 266 to ca. 3 after 10 minutes of discharge. The sole plasma discharge is reported to produce ozone,  
 267 hydroxyl radicals, reactive oxygen and nitrogen species (Perinban et al., 2019). Hydroxyl radicals in  
 268 the liquid suspension during plasma treatment in the absence of UVA light could not be detected  
 269 through benzoic acid-based trapping methods (Vione et al., 2010; Berardinelli et al. 2021). Production



270 of ozone has been elsewhere reported for this system in the dark (Ragni et al., 2016). Therefore,  
271 plasma induced oxidation of MB can be at this stage of investigation tentatively attributed to ozone  
272 or to ROS and RNS dissolved in solution.

273 On the other hand, the degradation rate enhancement observed when plasma and UVA light operate  
274 simultaneously, can be attributed to dissolved species absorbing in the emission range of the UVA  
275 lamps. Even if the effect of ozone in the dark cannot be neglected (Camera Roda et al., 2019), it  
276 cannot be responsible for the light induced enhancement as it presents an absorption shoulder centered  
277 at 254 nm, while wavelengths shorter than 300 nm are cut off by the Pyrex walls of the discharge  
278 chamber. Therefore, the intensification effect of the coupled UVA-plasma treatment must be related  
279 to the presence of ROS and/or RNS generated through plasma discharge, which are photoactive in  
280 the UVA range.

281 In order to unveil the nature of the synergistic effects between plasma and UVA irradiation, we carried  
282 out plasma, UVA, and combined plasma-UVA treatments in the presence of phenylalanine (PA). The  
283 choice of this compound relies firstly on its biological nature, which makes it suitable for the purposes  
284 of this investigation. Moreover, phenylalanine is a known trap molecule for ROS and RNS species  
285 (Oeckl and Ferger, 2009), producing three major hydroxylation (o-, m-, p-tyrosine) and two major  
286 nitration products (nitrophenylalanine, nitrotyrosine) as shown in Fig. 4. In particular, the presence  
287 of these reaction intermediates has also been used in literature to infer the presence of peroxynitrous  
288 species (van der Vliet et al., 1994).

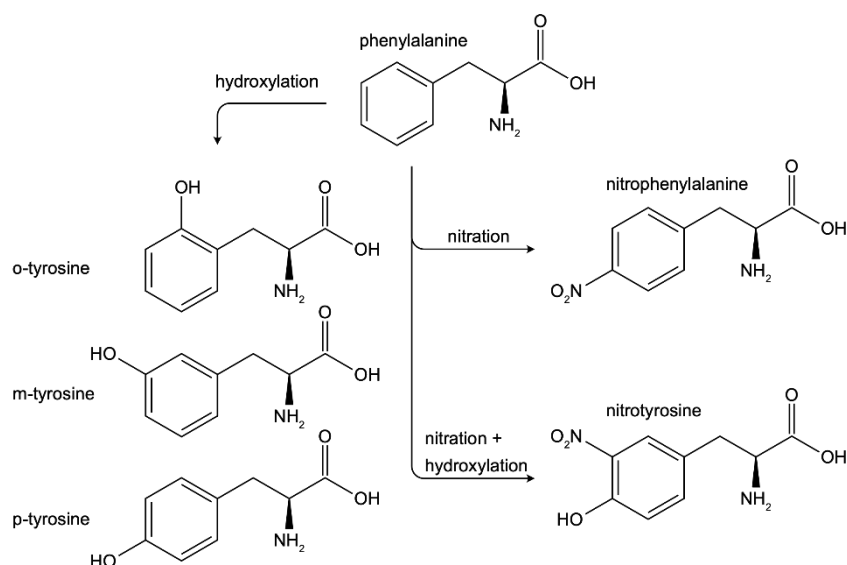


**Fig. 4.** Products of nitration and/or hydroxylation of phenylalanine (PA).

Fig. 5a shows the normalized concentration of PA during time for UVA, plasma and coupled UVA-plasma treatment, while Fig. 5b and 5c report the formation of tyrosine (TYR) and para-nitrophenylalanine (NPA), respectively, for the same runs. The concentration of tyrosine is calculated as the sum of the concentrations of the three isomers (ortho, meta and para). No nitrotyrosine could be detected during the 60-minute runs. In addition, during the PA degradation tests in the presence of cold plasma, the pH of the solution decreased to ca. 3 after 10 minutes from switching on the discharge.

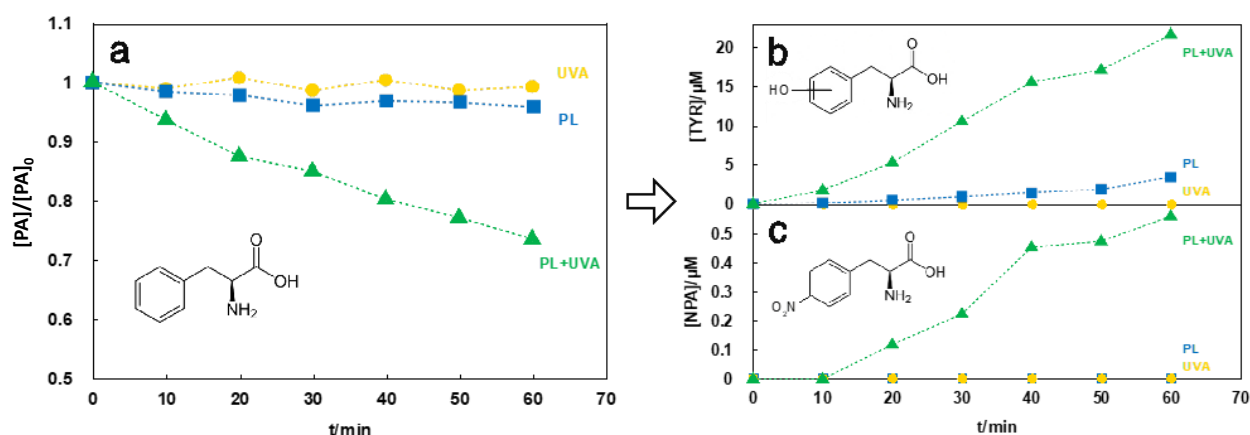


**Fig. 5.** Normalized concentration of phenylalanine (a), concentration of generated tyrosine (b) and nitrophenylalanine (c) during UV light (UVA, yellow circles), cold plasma (PL, blue squares), and integrated UV light – cold plasma (PL + UVA, green triangles) treatment. Each reaction was performed three times and the standard deviation was  $\pm 5\%$ .

Sole UVA irradiation does not produce degradation of phenylalanine and, accordingly, no reaction products were detected in this case. This result is in agreement with the fact that PA does not absorb at wavelengths longer than 300 nm. In the presence of the sole plasma discharge, phenylalanine degradation proceeds to a certain extent, and formation of tyrosine could be observed. In this case traces of nitrophenylalanine could be detected only after 120 minutes of plasma treatment (not reported in Fig. 5c). When combining cold plasma and UVA irradiation, significant degradation of phenylalanine can be observed and, accordingly, the production of tyrosine is increased seven-fold with respect to the case of sole plasma treatment. Moreover, under these conditions formation of nitrophenylalanine could be also observed already during the first 60 minutes of treatment (Fig. 5c). Results show that formation of hydroxylation and nitration intermediates is greatly amplified when UVA and plasma processes act simultaneously. Notably, the observed effect holds also in terms of energy consumption, as shown in Fig. S4 (Supporting information). The faster degradation retrieved

also on a per-unit energy basis is relevant in perspective for a possible scale-up of the process, as recently highlighted in literature (Wang et al., 2021; Wang et al., 2022).

Among the post discharge species formed in plasma activated water, peroxyntrous acid is reported in literature along with hydrogen peroxide, ozone, nitrate and nitrite ion, and superoxide radical (Perinban et al., 2019). However, while plenty of information are available in literature on the latter species, quantitative data on peroxyntrous acid formation have been rarely reported (Tarabova et al., 2019). In order to get direct and quantitative evidence of the presence of peroxyntrous acid in plasma activated water, with and without UVA irradiation, we performed the measurement as described in the experimental part. Results are shown in Fig. 6.

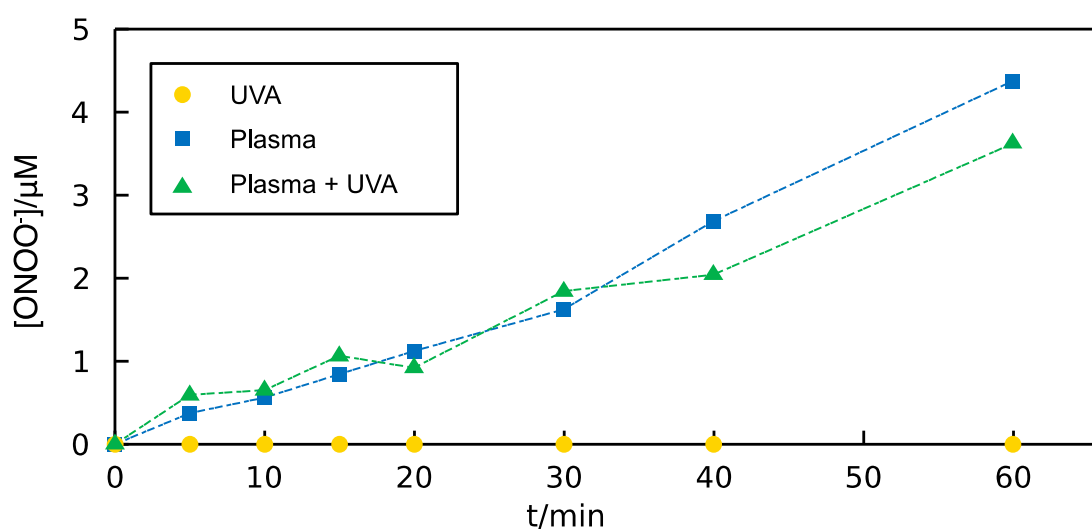
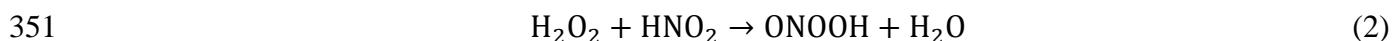
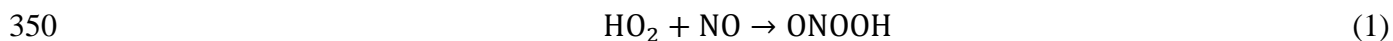


**Fig. 6.** Time dependence of the concentration of peroxyntrous acid in plasma activated water (measured as peroxyntrite ion upon alkalization of the sample) in the absence (blue squares) and in the presence (green triangles) of UVA irradiation. Results under sole UVA irradiation are also reported (yellow circles). Each test have been performed three times and the standard deviation was  $\pm 5\%$ .

The concentration of peroxyntrous acid in plasma activated water increases almost linearly during the discharge, reaching a concentration of ca. 4  $\mu\text{M}$  after 60 minutes of plasma glowing. It is worth

337 to mention that this value could underestimate the real concentration in plasma activated water, due  
338 to the few seconds needed to transfer the solution into the NaOH solution. However, the error results  
339 systematic, due to the standardized procedure of measurement. Notably, formation of peroxyntrous  
340 acid does not depend on the simultaneous UVA irradiation. Even if apparently this result seems to  
341 disagree with the intensification effect observed, we have to consider that the measurement is carried  
342 out in distilled water. In fact, peroxyntrous acid is a transient species, whose concentration is the  
343 result of equilibria greatly influenced by the presence of dissolved molecules such as phenylalanine.  
344 However, the direct evidence of the formation of peroxyntrous acid in plasma activated water, along  
345 with the results of the biological and chemical tests described above, allows to propose some  
346 mechanistic insights on the observed synergistic effects.

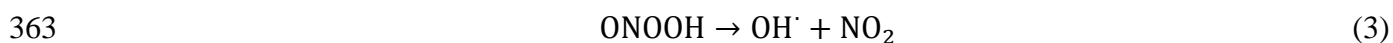
347 Peroxyntrous acid (ONOOH) is an unstable isomer of nitric acid, which can be produced through  
348 reaction of superoxide radicals and nitrogen oxide (Eq. (1)) (Pryor and Squadrito, 1995), or by  
349 reaction of hydrogen peroxide and nitrous acid (Eq. (2)) (Saha et al., 1998).



352 All of the reactants in Eqs. 1-2 are reported to be post discharge species present in plasma activated  
353 water (Perinban et al., 2019). By taking into account that the pH of plasma activated water reaches a  
354 value of ca. 3 after few minutes, peroxyntrous acid is present mainly in its protonated form (ONOOH,  
355  $\text{pK}_a = 6.8$ ) (Pryor and Squadrito, 1995).

356 Despite decades of research, a complete understanding of the chemistry of peroxyntrous acid has  
357 proved to be elusive (Koppenol et al., 2012). Peroxyntrous acid is reported to quickly isomerize to  
358 nitric acid. However, in the presence of suitable substrates such as phenylalanine, is reported to give  
359 rise to hydroxylation and nitration directly (Goldstein et al., 1996), or indirectly after homolytic  
360 rupture of the O-O bond and consequent formation of hydroxyl radical and nitrogen dioxide (Eq. (3)),

361 which in turn can initiate hydroxylation and nitration reactions, respectively (Pryor and Squadrito,  
362 1995).



364 Even if the homolysis of ONOOH and the mechanism of isomerization to nitric acid are still under  
365 debate in literature (Koppenol et al., 2012), there is agreement on the hydroxylating and nitrating  
366 capability of peroxynitrous acid.

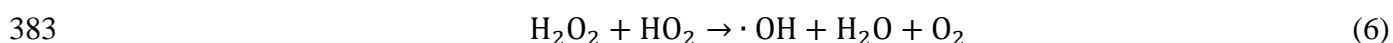
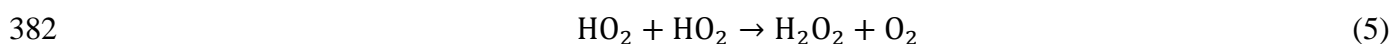
367 It shall be mentioned that another pathway of decomposition of peroxynitrous acid has been reported  
368 (Eq. (4)), where the products are oxygen and nitrite



370 However, the kinetics of this mechanism is negligible at a pH below 4 (Coddington et al., 1999),  
371 which is the case of the present experimental conditions.

372

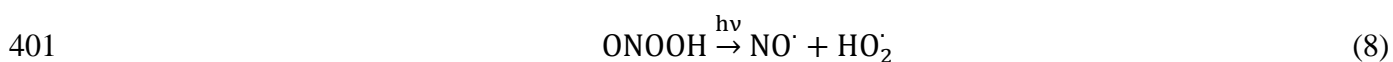
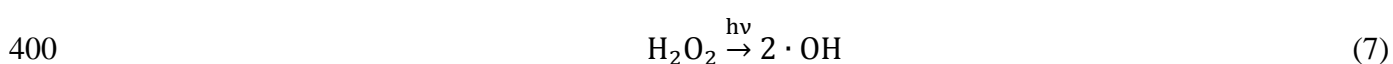
373 The formation of small amounts of tyrosine and traces of nitrophenylalanine observed with the plasma  
374 treatment in dark conditions can be hardly attributed to the sole action of peroxynitrous acid. The  
375 limited extent to which phenylalanine was converted suggests that the action of peroxynitrous acid is  
376 relatively modest. The short life of peroxynitrous acid can readily account for that, as confirmed by  
377 the relevant amount of nitrate detected in plasma activated water. Moreover, several other post-  
378 discharge reactions could be responsible for the tyrosine formed after plasma discharge under dark  
379 conditions. Primarily, hydroxylation can be induced by hydroxyl radicals directly generated by  
380 plasma, or formed by known reaction of superoxide radicals ( $\text{HO}_2$ ) in water (Parrino et al., 2015)  
381 (Eqs. 5-6).



384 It shall be mentioned that generation of hydroxyl radicals is also reported through reaction between  
 385 ozone and hydrogen peroxide (known as the *peroxone* process). However, this reaction requires  
 386 deprotonated hydrogen peroxide (pKa ~12) (Merényi et al., 2010), thus is inefficient at acidic pH  
 387 values (Ding et al., 2019). Finally, the plasma discharge emits some UV radiation. Therefore, it  
 388 cannot be excluded that some of the reactions discussed below under UVA irradiation could take  
 389 place even under nominal dark conditions.

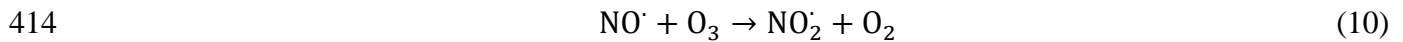
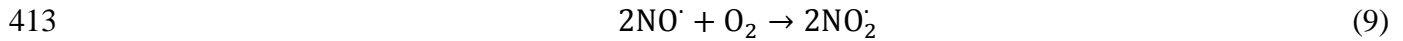
390

391 Under external UVA irradiation of plasma activated water, both hydroxylation and nitration products  
 392 are formed, and faster degradation of phenylalanine is observed (Fig. 5). Hydroxyl radicals can be  
 393 formed directly through photolysis of hydrogen peroxide, occurring at wavelengths shorter than 400  
 394 nm (Eq. (7)). On the other hand, hydroxyl radicals can be indirectly produced through photolysis of  
 395 peroxyntous acid (at  $\lambda < 355$  nm) to nitrogen oxide and hydroperoxyl radical (Eq. (8)). Accordingly,  
 396 Sturzbecher et al., 2009 reports that photolysis of peroxyntous acid occurs primarily (95%) through  
 397 fast homolytic rupture of the N-O bond with a rate constant of  $1.6 \times 10^{10} \text{ M}^{-1} \text{ s}^{-1}$ . Hydroperoxyl  
 398 radicals ( $\text{OH}_2$ ) in turn, produce hydrogen peroxide according to Eq. (5), thus becoming a further  
 399 source of hydroxyl radicals (Eq. (6)-(7)).

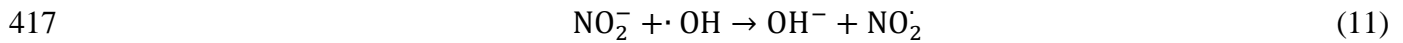


402 Therefore, hydroxyl radicals are eventually generated by photolysis of hydrogen peroxide, deriving  
 403 directly from plasma discharge or indirectly from photolysis of peroxyntous acid (Eq. (5)-(6), (8)).  
 404 The presence of nitrophenylalanine, detected after the first minutes of reaction only in the UVA-  
 405 plasma integrated process, suggests that the contribution of peroxyntous acid to the process  
 406 intensification observed under UVA irradiation of plasma activated water is not negligible. In fact,  
 407 the sole plasma discharge produces only traces of nitrophenylalanine, indicating that the direct  
 408 nitration through peroxyntous acid reported in literature (van der Vliet et al., 1994) is a secondary

409 path also under UVA irradiation. On the other hand, it seems more plausible to consider nitrogen  
410 oxide produced upon photolysis of peroxyxynitrous acid (Eq. (8)) as a source of NO<sub>2</sub>, which is a known  
411 nitrating agent (Beckman and Koppenol, 1996). In fact, NO<sub>2</sub> can be easily produced by reaction of  
412 nitrogen monoxide with either oxygen (Eq. (9)) or ozone (Eq. (10)) (Fontijn et al., 1970).



415 Finally, a further source of NO<sub>2</sub> under UVA irradiation could be the reaction of hydroxyl radicals  
416 with nitrite ions (Eq. (11)) (Coddington et al., 1999).



418 This path could contribute to nitration under UVA irradiation due to the enhanced production of  
419 hydroxyl radicals above mentioned. However, the rate constant reported in literature for this reaction  
420 is almost one order of magnitude lower than the photolysis of peroxyxynitrous acid (Eq. (8)) which,  
421 therefore, seems to play a key role, together with hydrogen peroxide, in the intensification effect  
422 observed when irradiating plasma activated water.

423 In order to test if plasma treatment alone or under simultaneous UVA irradiation affects the quality  
424 parameters of fish fillet, we investigated color and sensorial attributes during storage for five days.  
425 Main results are reported in the Supporting Information (Table S1) in terms of L\* and C\* values and  
426 demerit scores mean values and standard deviations.

427 In general, for both color attributes, slight differences (p-level < 0.05) between the control sample  
428 and sample means characterized by different storage days were observed for both plasma and plasma  
429 with UVA treatments. A slight increase in lightness was observed immediately after the treatments  
430 and for the control samples. This result was probably because all samples (treated and control) were  
431 immersed in 200 mL of distilled water (Trevisani et al., 2021). This last effect was not appreciated in  
432 terms of demerit score that, as expected, increases by increasing the storage days due to degradative  
433 mechanisms normally observed during fish fillet shelf life (Cheng et al., 2015).



434 Main results suggest that the proposed treatments do not induce appreciable modifications in the  
435 quality attributes with respect to a control sample during the shelf life of five days at 4°C.

436

#### 437 **4. Conclusions**

438 Low energy “cold plasma” generated in a confined chamber through dielectric barrier discharge has  
439 been demonstrated to degrade chemical compounds and to reduce *L. monocytogenes* in aqueous  
440 solution. UVA light alone, being far less energetic than the commonly used germicidal UVC light,  
441 does not provide neither chemical degradation nor bacterial inactivation. However, the simultaneous  
442 irradiation of the reacting substrate with UVA light irradiation significantly enhances the efficiency  
443 of chemical degradation and microbial reduction, in the integrated process with respect to the sole  
444 plasma treatment. Degradation tests with phenylalanine, a known peroxynitrous acid trap and the  
445 quantitative evaluation of the amount of peroxynitrous acid produced during plasma treatment  
446 allowed to highlight the role of peroxynitrous acid in the synergistic effect observed. The integrated  
447 plasma-UVA process does not affect the quality parameters of fish fillet samples subjected to the  
448 treatment. Therefore, these results could potentially boost a commercial diffusion of plasma devices  
449 for food applications in liquid phase, which have been up to now hindered by the limited penetration  
450 of short living gaseous reactive species into the deeper layers of bulky food products.

451

#### 452 **Acknowledgements**

453 This research did not receive any specific grant from funding agencies in the public, commercial, or  
454 not-for-profit sectors.

455 **Index of Figures**

456 **Fig. 1.** Scheme of the experimental set up consisting of the dielectric barrier discharge (DBD) device  
457 in a Pyrex chamber surrounded by UVA lamps.

458 **Table 1.** Demerit score scheme for sensory evaluation.

459 **Fig. 2.** Cell viability of *Listeria monocytogenes* 56Ly cells in saline solution and pH values of the  
460 solutions after exposure for 60 min to UV light (UVA), cold plasma (PL), and integrated UV light –  
461 cold plasma (PL + UVA) treatments. Values represent means  $\pm$  standard deviations of values from  
462 three separate experiments. Different letters indicate significant differences among treatments ( $p <$   
463 0.05, ANOVA, post hoc Tukey).

464 **Fig. 3.** Normalized concentration of methylene blue (MB) during UVA light (UVA, circles), UV light  
465 in the presence of 1 mM sodium nitrite (UVA+nitrite, X marks), cold plasma (PL, squares), and  
466 integrated UVA light – cold plasma (PL + UVA, triangles) treatment. Each reaction was performed  
467 three times and the standard deviation was  $\pm 5\%$ . Significant differences among treatments were  
468 observed at each treatment time ( $p < 0.05$ , Mann-Whitney test).

469 **Fig. 4.** Products of nitration and/or hydroxylation of phenylalanine (PA).

470 **Fig. 5.** Normalized concentration of phenylalanine (A), concentration of generated tyrosine (B) and  
471 nitrophenylalanine (C) during UV light (UVA, yellow circles), cold plasma (PL, blue squares), and  
472 integrated UV light – cold plasma (PL + UVA, green triangles) treatment. Each reaction was  
473 performed three times and the standard deviation was  $\pm 5\%$ .

474 **Fig. 6.** Time dependence of the concentration of peroxynitrous acid in plasma activated water  
475 (measured as peroxynitrite ion upon alkalization of the sample) in the absence (blue squares) and  
476 in the presence (green triangles) of UVA irradiation. Results under sole UVA irradiation are also  
477 reported (yellow circles). Each test have been performed three times and the standard deviation was  
478  $\pm 5\%$ .

479

480

481     **References**

- 482     Andoni, E., Ozuni, E., Bijo, B., Shehu, F., Branciari, R., Miraglia, D., et al., 2021. Efficacy of non-  
483     thermal processing methods to prevent fish spoilage. *J. Aquat. Food Prod. Technol.* 30, 228–245.  
484     <https://doi.org/10.1080/10498850.2020.1866131>.
- 485     Beckman, J. S., Koppenol, W. H., 1996. Nitric oxide, superoxide, and peroxynitrite: the good, the  
486     bad, and ugly. *Am. J. Physiol. Cell Physiol.* 271, C1424-C1437.  
487     <https://doi.org/10.1152/ajpcell.1996.271.5.C1424>.
- 488     Berardinelli, A., Vannini, L., Ragni, L., Guerzoni, M. E., 2012. Impact of Atmospheric Plasma  
489     Generated by a DBD Device on Quality-Related Attributes of “Abate Fetel” Pear Fruit, in:  
490     Machala, Z., Hensel, K., Akishev, Y. (Eds.), *Plasma for Bio-Decontamination, Medicine and Food*  
491     *Security. NATO Sci. for Peace and Secur. Ser. A: Chem. and Biol.* Springer, Dordrecht.  
492     [https://doi.org/10.1007/978-94-007-2852-3\\_35](https://doi.org/10.1007/978-94-007-2852-3_35).
- 493     Berardinelli, A., Pasquali, F., Cevoli, C., Trevisani, M., Ragni, L., Mancusi, R., Manfreda, G.,  
494     2016. Sanitisation of fresh-cut celery and radicchio by gas plasma treatments in water medium.  
495     *Postharvest Biol. Technol.* 111, 297–304. <https://doi.org/10.1016/j.postharvbio.2015.09.026>.
- 496     Berardinelli, A., Hamrouni, A., Dirè, S., Ceccato, R., Camera-Roda, G., Ragni, L., et al., 2021.  
497     Features and application of coupled cold plasma and photocatalysis processes for decontamination  
498     of water. *Chemosphere.* 262, 128336. <https://doi.org/10.1016/j.chemosphere.2020.128336>.
- 499     Bourke, P., Ziuzina, D., Han, L., Cullen, P. J., Gilmore, B. F., 2017. Microbiological interactions  
500     with cold plasma. *J. Appl. Microbiol.* 123, 308-324. <https://doi.org/10.1111/jam.13429>.

501 Camera-Roda, G., Loddo, V., Palmisano, L., Parrino, F., 2019. Photocatalytic ozonation for a  
 502 sustainable aquaculture: a long-term test in a seawater aquarium. *Appl. Catal. B.* 253, 69-76.  
 503 <https://doi.org/10.1016/j.apcatb.2019.04.048>.

504 Cardenas Bonilla, A., Sveinsdottir, K. and Martinsdottir, E., 2007. Development of quality index  
 505 method (QIM) scheme for fresh cod (*gadus morhua*) fillets and application in shelf life study. *Food*  
 506 *Control.* 18, 352–358. <https://doi.org/10.1016/j.foodcont.2005.10.019>.

507 Cheng, J.-H., Sun, D.-W., Zeng, X.-A., Liu, D., 2015. Recent advances in methods and techniques  
 508 for freshness quality determination and evaluation of fish and fish fillets: a review. *Crit. Rev. Food*  
 509 *Sci. Nutr.* 55, 1012–1225. <https://doi.org/10.1080/10408398.2013.769934>.

510 Chowdhury, P., Viraraghavan, T., Srinivasan, A., 2010. Biological treatment processes for fish  
 511 processing wastewater – A review. *Bioresour. Technol.* 101, 439–449.  
 512 <https://doi.org/10.1016/j.biortech.2009.08.065>.

513 Coddington, J., Hurst, J. K., Lyman, S. V., 1999. Hydroxyl radical formation during peroxyntous  
 514 acid decomposition. *J. Am. Chem. Soc.* 121, 2438–2443.

515 Dezest, M., Bulteau, A.L., Quinton, D., Chavatte, L., Le Behec, M., Cambus, J.P., Arbault, S.,  
 516 Nègre-Salvayre, A., Clement, F., Cousty, S., 2017. Oxidative modification and electrochemical  
 517 inactivation of *Escherichia coli* upon cold atmospheric pressure plasma exposure. *PLoS ONE.* 12,  
 518 e0173618. <https://doi.org/10.1371/journal.pone.0173618>.

519 Ding, Y., Bao, H., Qian, R., Shen, T., Tong, S., 2019. N-Graphene-CeO<sub>2</sub> nanocomposite enriched  
 520 with Ce (III) sites to improve the efficiency of peroxone reaction under acidic conditions. Sep.  
 521 Purif. Technol. 225, 80–87. <https://doi.org/10.1016/j.seppur.2019.05.065>.

522 EFSA Journal, 2019. Chemical risks associated with ready-to-eat vegetables: quantitative analysis  
 523 to estimate formation and/or accumulation of disinfection byproducts during washing. 17(S2):  
 524 e170913.

525 Ekonomou, S. I., Boziaris, I. S., 2021. Non-thermal methods for ensuring the microbiological  
 526 quality and safety of seafood. Appl. Sci. 11. <https://doi.org/10.3390/app11020833>.

527 Fitzhenry, K., Barrett, M., O'Flaherty, V., Dore, W., Cormican, M., Rowan, N., et al., 2016. The  
 528 Effect of Wastewater Treatment Processes, in Particular Ultraviolet Light Treatment, on Pathogenic  
 529 Virus Removal. EPA research, report n 171.

530 Fontijn, A., Sabadell, A. J., Ronco, R. J., 1970. Homogeneous chemiluminescent measurement of  
 531 nitric oxide with ozone. Implications for continuous selective monitoring of gaseous air pollutants.  
 532 Anal. Chem. 42, 575–579. <https://doi.org/10.1021/ac60288a034>.

533 Gil, M.I., Selma, M.V., López-Gálvez, F., Allende, A., 2009. Fresh-cut product sanitation and  
 534 wash water disinfection: problems and solutions. Int. J. Food Microbiol. 134, 37–45.  
 535 <https://doi.org/10.1016/j.ijfoodmicro.2009.05.021>.

536 Goldstein, S., Squadrito, G. L., Pryor, W. A., Czapski, G., 1996. Direct and indirect oxidations by  
 537 peroxynitrite, neither involving the hydroxyl radical. Free Radic. Biol. Med. 21, 965–974.  
 538 [https://doi.org/10.1016/S0891-5849\(96\)00280-8](https://doi.org/10.1016/S0891-5849(96)00280-8).

539 Guo, J., Huang, K., Wang, J., 2015. Bactericidal effect of various non-thermal plasma agents and  
 540 the influence of experimental conditions in microbial inactivation: A review. *Food Control*. 50,  
 541 482–490. <https://doi.org/10.1016/j.foodcont.2014.09.037>.

542 Hughes, M. N., Nicklin, H. G., 1968. The chemistry of pernitrites. Part I. Kinetics of decomposition  
 543 of pernitrous acid. *J. Chem. Soc. A*. 450–452. <https://doi.org/10.1039/J19680000450>.

544 Jeon, M-J., Ha, J-W., 2020. Inactivating foodborne pathogens in apple juice by combined treatment  
 545 with fumaric acid and ultraviolet-A light, and mechanisms of their synergistic bactericidal action.  
 546 *Food Microbiol.* 87, 103387. <https://doi.org/10.1016/j.fm.2019.103387>.

547 Jiang B., Zheng J., Wu M, 2016. Nonthermal Plasma for Effluent and Waste Treatment, in: Misra,  
 548 N. N., Schlüter, O., Cullen, P.J. (Eds.), *Cold Plasma in Food and Agriculture: Fundamentals and*  
 549 *Applications*. Elsevier Inc., Amsterdam. <https://doi.org/10.1016/B978-0-12-801365-6.00013-5>.

550 Koppenol, W. H., Bounds, P. L., Nauser, T., Kissner, R., Rügger, H., 2012. Peroxynitrous acid:  
 551 controversy and consensus surrounding an enigmatic oxidant. *Dalton Trans.* 41, 13779–13787.  
 552 <https://doi.org/10.1039/c2dt31526b>.

553 Kulawik, P., Tiwari, B. K., 2019. Recent advancements in the application of non-thermal plasma  
 554 technology for the seafood industry. *Crit. Rev. Food Sci. Nutr.* 59, 3199–3210.  
 555 <https://doi.org/10.1080/10408398.2018.1510827>.

556 Meireles, A., Giaouris, E., Simões, M., 2016. Alternative disinfection methods to chlorine for use in  
 557 the fresh-cut industry. *Food Res. Int.* 82, 71–85. <https://doi.org/10.1016/j.foodres.2016.01.021>.

558 Merényi, G., Lind, J., Naumov, S., Sonntag, C. v., 2010. Reaction of ozone with hydrogen peroxide  
 559 (peroxone process): a revision of current mechanistic concepts based on thermokinetic and  
 560 quantum-chemical considerations. *Environ. Sci. Technol.* 44, 3505–3507.  
 561 <https://doi.org/10.1021/es100277d>.

562 Miklos, D. B., Remy, C., Jekel, M., Linden, K. G., Drewes, J. E., Hübner, U., 2018. Evaluation of  
 563 advanced oxidation processes for water and wastewater treatment – A critical review. *Water Res.*  
 564 139, 118–131. <https://doi.org/10.1016/j.watres.2018.03.042>.

565 Mitoraj, D., Umaporn, L., Wiyong, K., Pacia, M., Macyk, W., Wetchakun N., Beranek, R., 2018.  
 566 Revisiting the problem of using methylene blue as a model pollutant in photocatalysis: The case of  
 567  $\text{InVO}_4/\text{BiVO}_4$  composites. *J. Photochem. Photobiol. A.* 366, 103–110.  
 568 <https://doi.org/10.1016/j.jphotochem.2018.02.023>.

569 Montie, T. C., Kelly-Wintenberg, K., Roth, J. R., 2000. An overview of research using the one  
 570 atmosphere uniform glow discharge plasma (OAUGDP) for sterilization of surfaces and materials.  
 571 *IEEE Trans. Plasma Sci.* 28, 41–50. <https://doi.org/10.1109/27.842860>.

572 Moreau, M., Orange, N., Feuilleux, M. G. J., 2008. Non-thermal plasma technologies: new tools  
 573 for bio-decontamination. *Biotechnol. Adv.* 26, 610–617.  
 574 <https://doi.org/10.1016/j.biotechadv.2008.08.001>.

575 Murali, S., Krishnan, V. S., Amulya, P. R., Alfiya, P. V., Delfiya, D. S. A., Samuel, M. P., 2021.  
 576 Energy and water consumption pattern in seafood processing industries and its optimization  
 577 methodologies. *Clean. Eng. Technol.* 4, 100242. <https://doi.org/10.1016/j.clet.2021.100242>.

578 Oeckl, P., Ferger, B., 2009. Analysis of hydroxylation and nitration products of d-phenylalanine for  
 579 in vitro and in vivo radical determination using high-performance liquid chromatography and  
 580 photodiode array detection. *J. Chromatogr. B.* 877, 1501–1508.  
 581 <https://doi.org/10.1016/j.jchromb.2009.03.031>.

582 Oehmigen, K., Hahnel, M., Brandenburg, R., Wilke, Ch., Weltmann, K.D., von Woedtke, Th.,  
 583 2010. The role of acidification for antimicrobial activity of atmospheric pressure plasma in liquids.  
 584 *Plasma Process. Polym.* 7, 250–257. <https://doi.org/10.1002/ppap.200900077>.

585 Parrino, F., Camera-Roda, G., Loddo, V., Augugliaro, V., Palmisano, L., 2015. Photocatalytic  
 586 ozonation: maximization of the reaction rate and control of undesired by-products. *Appl. Catal. B.*  
 587 178, 37–43. <https://doi.org/10.1016/j.apcatb.2014.10.081>.

588 Parrino, F., Livraghi, S., Giamello, E., Ceccato, R., Palmisano, L., 2020. Role of hydroxyl,  
 589 superoxide, and nitrate radicals on the fate of bromide ions in photocatalytic TiO<sub>2</sub> suspensions.  
 590 *ACS Catal.* 10, 7922–7931. <https://doi.org/10.1021/acscatal.0c02010>.

591 Pavlovich, M.J., Sakiyama, Y., Clark, D.S., Graves, D.B., 2013. Antimicrobial synergy between  
 592 ambient-gas plasma and UVA treatment of aqueous solution. *Plasma Process. Polym.* 10, 1051–  
 593 1060. <https://doi.org/10.1002/ppap.201300065>.

594 Perinban, S., Orsat, V., Raghavan, V., 2019. Nonthermal plasma–liquid interactions in food  
 595 processing: a review. *Compr. Rev. Food Sci. Food Saf.* 18, 1985–2008.  
 596 <https://doi.org/10.1111/1541-4337.12503>.



597 Probst-Rüd, S., McNeill, K., Ackermann, M., 2017. Thiouridine residues in tRNAs are responsible  
 598 for a synergistic effect of UVA and UVB light in photoinactivation of *Escherichia coli*. *Environ.*  
 599 *Microbiol.* 19, 434–442. <https://doi.org/10.1111/1462-2920.13319>.

600 Pryor, W. A., Squadrito, G., 1995. The chemistry of peroxynitrite: a product from the reaction of  
 601 nitric oxide with superoxide. *Am. J. Physiol.* 268, L699–722.  
 602 <https://doi.org/10.1152/ajplung.1995.268.5.L699>.

603 Ragni, L., Berardinelli, A., Iaccheri, E., Gozzi, G., Cevoli, C., Vannini, L., 2016. Influence of the  
 604 electrode material on the decontamination efficacy of dielectric barrier discharge gas plasma  
 605 treatments towards *Listeria monocytogenes* and *Escherichia coli*. *Innov. Food Sci. Emerg. Technol.*  
 606 37, 170–176. <https://doi.org/10.1016/j.ifset.2016.07.029>.

607 Saha, A., Goldstein, S., Cabelli, D., Czapski, G., 1998. Determination of optimal conditions for  
 608 synthesis of peroxynitrite by mixing acidified hydrogen peroxide with nitrite. *Free Radic. Biol.*  
 609 *Med.* 24, 653–659. [https://doi.org/10.1016/S0891-5849\(97\)00365-1](https://doi.org/10.1016/S0891-5849(97)00365-1).

610 Sampels, S., 2014. Towards a more sustainable production of fish as an important protein source for  
 611 human nutrition. *J. Fish. Livest. Prod.* 2, 119. <https://doi.org/10.4172/2332-2608.1000119>.

612 Sefa-Dedeh, S., 2003. Traditional Food Technology, in: Caballero, B., (Ed.), *Encyclopedia of Food*  
 613 *Sciences and Nutrition*. Academic Press, Cambridge, MA., pp. 5828–5834.  
 614 <https://doi.org/10.1016/B0-12-227055-X/01205-0>.

615 Sturzbecher-Höhne, M., Nauser, T., Kissner, R., Koppenol, W. H., 2009. Photon-initiated  
 616 homolysis of peroxynitrous acid. *Inorg. Chem.* 48, 7307–7312. <https://doi.org/10.1021/ic900614e>.

617 Tarabová, B., Lukeš, P., Hammer, M. U., Jablonowski, H., von Woedtke, T., Reuter, S., Machala,  
 618 Z., 2019. Fluorescence measurements of peroxynitrite/peroxynitrous acid in cold air plasma treated  
 619 aqueous solutions. *Phys. Chem. Chem. Phys.* 21, 8883-8896. <https://doi.org/10.1039/c9cp00871c>.

620 Trevisani, M., Cevoli, C., Ragni, L., Cecchini, M., Berardinelli, A., 2021. Effect of non-thermal  
 621 atmospheric plasma on viability and histamine-producing activity of psychotrophic bacteria in  
 622 mackerel fillets. *Front. Microbiol.* 12. <https://doi.org/10.3389/fmicb.2021.653597>.

623 UNEP, United Nations Environment Programme, 1999. Cleaner production assessment in fish  
 624 processing. UNEP, Division of Technology, Industry and Economics. Paris.

625 Vione, D., Ponzo, M., Bagnus, D., Maurino, V., Minero, C., Carlotti, M. E., 2010. Comparison of  
 626 different probe molecules for the quantification of hydroxyl radicals in aqueous solution. *Environ.*  
 627 *Chem. Lett.* 8, 95–100. <https://doi.org/10.1007/s10311-008-0197-3>.

628 Van der Vliet, A., O'Neill, C. A., Halliwell, B., Cross, C. E., Kaur, H., 1994. Aromatic  
 629 hydroxylation and nitration of phenylalanine and tyrosine by peroxynitrite. Evidence for hydroxyl  
 630 radical production from peroxynitrite. *FEBS Lett.* 339, 89–92.  
 631 [https://doi.org/10.1016/0014-5793\(94\)80391-9](https://doi.org/10.1016/0014-5793(94)80391-9).

632 Wang, D., Mueses, M. A., Márquez, J. A. C., Machuca-Martínez, F., Grčić, I., Moreira, R., Li  
 633 Puma, G., 2021. Engineering and modeling perspectives on photocatalytic reactors for water  
 634 treatment. *Water Res.* 202, 117421. <https://doi.org/10.1016/j.watres.2021.117421>.

635 Wang, D., Junker, A. L., Sillanpää, M., Jiang, Y., Wei, Z., 2022. Photo-based advanced oxidation  
 636 processes for zero pollution: where are we now? *Eng.* <https://doi.org/10.1016/j.eng.2022.08.005>.